Available online at www.sciencedirect.com
SCIENCE DIRECT®
ELSEVIER
Nuclear Instruments and Methods in Physics Research A 544 (2005) 514–519
NUCLEAR INSTRUMENTS & METHODS IN PHYSICS RESEARCH Section A
www.elsevier.com/locate/nima

# Laser-Induced Fluorescence diagnostic of barium ion plasmas in the Paul Trap Simulator Experiment

Moses Chung*, Erik P. Gilson, Ronald C. Davidson, Philip C. Efthimion, Richard Majeski, Edward A. Startsev

*Plasma Physics Laboratory, Princeton University, Princeton, NJ 08543, USA*

Available online 7 March 2005

**Abstract**

The Paul Trap Simulator Experiment (PTSX) is a cylindrical Paul trap whose purpose is to simulate the nonlinear dynamics of intense charged particle beam propagation in alternating-gradient magnetic transport systems. To investigate the ion plasma microstate in PTSX, including the ion density profile and the ion velocity distribution function, a laser-induced fluorescence diagnostic system is being developed as a nondestructive diagnostic. Instead of cesium, which has been used in the initial phase of the PTSX experiment, barium has been selected as the preferred ion for the laser-induced fluorescence diagnostic. A feasibility study of the laser-induced fluorescence diagnostic using barium ions is presented with the characterization of a tunable dye laser. The installation of the barium ion source and the development of the laser-induced fluorescence diagnostic system are also discussed.


*PACS:* 41.75.Ak; 52.27.Jt; 39.10.+j; 42.62.Fi

*Keywords:* Ion beam; Plasma; Paul trap; Laser-induced fluorescence

## 1. Introduction

Periodic focusing accelerators and transport systems have applications ranging from basic scientific research in high energy and nuclear physics to applications such as coherent radiation generation, heavy ion fusion, tritium production, nuclear waste transmutation, and spallation neutron sources for material and biological research [1]. In order to provide a practically acceptable design of such experiments, the fundamental properties of space-charge-dominated beams must be well understood [2]. Through basic experimental studies, analytical investigations, and numerical simulation studies, considerable progress has been made in this area. Nonetheless, it remains important to develop an improved basic understanding of the nonlinear dynamics and collective processes in periodically focused intense charged

*Corresponding author.
*E-mail address:* mchung@princeton.edu (M. Chung).

0168-9002/$ - see front matter © 2005 Elsevier B.V. All rights reserved.
doi:10.1016/j.nima.2005.01.284

particle beams, with the goal of identifying operating regimes for stable beam propagation over hundreds, even thousands, of lattice periods of the periodic focusing magnetic field. Recently, Davidson et al. [3] proposed a design concept for a compact Paul trap experimental configuration that fully simulates the collective processes and nonlinear transverse dynamics of an intense charged particle beam that propagates over large distances through a periodic quadrupole magnetic field. Based on this idea, the Paul Trap Simulator Experiment (PTSX) device has been constructed at the Princeton Plasma Physics Laboratory (PPPL). Initial experiments on PTSX with a cesium ion source and a simple Faraday cup diagnostic have been very successful [4]. However, to investigate the detailed plasma microstate in PTSX, including the ion density profile and the ion velocity distribution function, a Laser-Induced Fluorescence (LIF) diagnostic system is proposed as a nondestructive measurement method. Because the atomic spectrum of barium is more amenable to LIF than cesium [5], barium has been selected as the preferred ion. This paper describes the progress to date in the development of LIF diagnostic system for PTSX and accompanying barium ion source.

## 2. PTSX device

The PTSX device has been described in detail elsewhere [4,6] and only a brief summary is given here. To generate the quadrupole electric field, the PTSX device is composed of cylindrical electrodes of radius $r_w = 10\,\text{cm}$ that are sliced into four $90^\circ$ azimuthal sectors. The central electrodes have length $2L = 2\,\text{m}$ while the end electrodes are each 40 cm long. The trap confines nonneutral ion plasmas radially by applying a periodic voltage $\pm V_0(t)$ with frequency $f$ to the four sectors of the central electrode, creating a ponderomotive force that is directed radially inwards. A DC voltage $+\hat{V}$ applied to the end electrodes confines the nonneutral ion plasma axially. The PTSX device manipulates the plasma using a load–trap–dump cycle. During loading (dumping), the short electrodes on the source (diagnostic) end are made to oscillate with the same voltages as the central electrodes. The typical operating pressure of PTSX is $5 \times 10^{-9}$ Torr.

## 3. Barium ion source

Barium ions are produced at the hot plate by contact ionization primarily in the ground state (6 $^2S_{1/2}$). However some fraction will be produced in the long-lived metastable state (5 $^2D_{3/2}$). The probability that an atom becomes ionized on a metal surface is

$$P_i = \left(1 + \frac{g_a}{g_i}\exp\{e(E-W)/k_B T\}\right)^{-1} \tag{1}$$

where $W$ and $T$ are the work function and temperature of the metal respectively, and $E$ is the ionization potential of the atom. The quantities $g_a$ and $g_i$ are statistical weights of the atoms and ions calculated from the total angular momentum quantum number. For example, for the alkali metals $g_a/g_i = 2$, and for the alkaline earths $g_a/g_i = 1/2$. In Q-machine experiments [7], rhenium has been used as a hot plate to produce barium ions by contact ionization and electrons by thermionic emission. But, in PTSX, where electrons are not present, platinum is a more favorable choice for the hot plate because of its lower operating temperature and higher work function. Bench tests on a test barium ion source with rhenium and platinum hot plates are being performed. Initial results show that currents up to 1 μA, which is sufficient for PTSX, can be obtained by using the platinum plate. A design for the barium ion source to be installed on PTSX is also being developed based on experiments done by Katsumata et al. [8] (Fig. 1).

## 4. Laser-induced fluorescence diagnostics

Fluorescence is observed when atoms and ions are excited to higher energy levels and then radiatively decay. The method based on this phenomenon, the LIF diagnostic, was first introduced to measure the ion velocity distribution

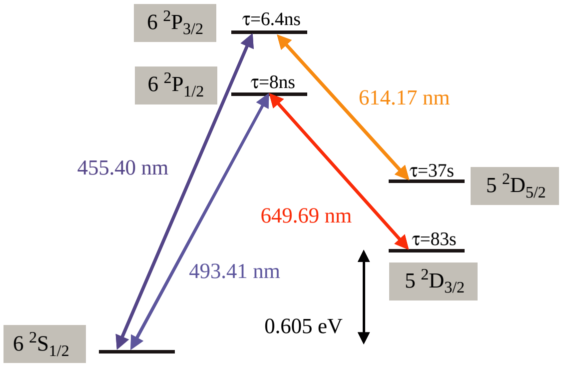


Fig. 1. Level diagram of $Ba^+$ with transition wavelengths and natural lifetimes [5].

function in an argon plasma 30 years ago, and has now become the most widely used laser diagnostic technique in many research fields. The LIF diagnostic is highly selective of species, and a very sensitive technique. Detection limits as low as $10^2$–$10^3$ particles/cm$^3$ have been reported under vacuum conditions by suppressing stray light [9]. Since the typical density of PTSX plasmas is $10^5$ particles/cm$^3$, and the background gas pressure is in the Ultrahigh Vacuum (UHV) range, there is no known physical limitation for LIF to be applied to PTSX plasmas. For the LIF diagnostic, a tunable laser is employed for a particular transition, exciting ions from an initial state to a higher energy state. The excited state rapidly decays (1–100 ns), emitting photons which are detected at 90° to the laser beam. Usually, the excitation and detection wavelengths are different to eliminate stray light by using an optical filter in front of the detector. However, in this case, the signal is reduced because the fluorescence is shared among different transitions. Furthermore, if there is a level with a long lifetime, particles can be trapped in this level and therefore cannot be re-excited.

In contrast to many other experiments which confine plasmas by external magnetic fields, PTSX does not utilize magnetic fields. Instead it uses oscillating electric fields to trap nonneutral ion plasmas. Hence, there is no Zeeman effect. But, a frequency shift in the LIF signals may be caused by the oscillating electric fields [10]. When the LIF signal is measured through a centrally located six-way cross, the DC electric fields from the end electrodes are quite small, and the self-electric field generated by the space-charge, which is of order $10^{-1}$ V/cm, can also be neglected. On the other hand, the AC electric field generated by the central electrodes can perturb the ion's atomic energy structure if the ion is displaced far from the center of the trap. But, because the time average electric field $\langle \mathbf{E} \rangle$ vanishes, Stark shifts which are linearly dependent on the electric field are absent. Since the magnitude of the AC electric field is of order $10$–$10^2$ V/cm in PTSX, the second-order Stark shift, which is quadratic in the electric field, is also expected to be small.

The usefulness of LIF as a diagnostic results from the fact that the intensity of the fluorescence signal, $I_{\mathrm{LIF}}$, is proportional to the population of the species in the excited state, and the excited state population is proportional to the population of the initial state before the laser is turned on. The latter is because the population dynamics of the states are simply governed by a set of linear homogeneous differential equations. In a three-level system, where the excited state can relax into a third state, the rate equations for the initial state ($n_1$) and the excited state ($n_2$), are given by [11]

$$\frac{\mathrm{d}n_1}{\mathrm{d}t} = -n_1 B_{12}\rho_\nu(\nu) + n_2 B_{21}\rho_\nu(\nu) + A_{21}n_2 \tag{2}$$

$$\frac{\mathrm{d}n_2}{\mathrm{d}t} = n_1 B_{12}\rho_\nu(\nu) - n_2 B_{21}\rho_\nu(\nu) - A_{21}n_2 - A_{23}n_2. \tag{3}$$

Because PTSX is operated in the collisionless regime, collisional transition terms are neglected here. The Einstein coefficients are related as follows:

$$g_1 B_{12} = g_2 B_{21} = g_2 A_{21}\frac{c^3}{8\pi h\nu^3} \tag{4}$$

where, $\rho_\nu(\nu) = I_\nu(\nu)/c[\mathrm{J/m^3\,Hz}]$ is the spectral energy density of a laser which has spectral width $\Delta\nu_{\mathrm{L}}$ around resonance frequency $\nu_0$. If $\Delta\nu_{\mathrm{L}}$ is large compared to the natural linewidth of the transition $\delta\nu_n = (A_{21} + A_{23})/2\pi$, the spectral laser intensity $I_\nu(\nu)[\mathrm{W/m^2\,Hz}]$ can be related to the total laser intensity $I[\mathrm{W/m^2}]$ by

$$I = \int I_\nu(\nu)\mathrm{d}\nu \approx I_\nu(\nu_0)\Delta\nu_\mathrm{L}. \tag{5}$$

From the rate equation for $n_2$, the maximum value of the excited state density can be estimated. This occurs when the laser intensity is sufficiently high that the stimulated emission dominates the spontaneous emission and the population of the third state is relatively small [12]. The dimensionless parameter that measures the ratio of stimulated emission to spontaneous emission is the saturation parameter $S$, which is given by

$$S = \frac{B_{21}\rho_\nu(\nu)}{A_{21}+A_{23}} = I\frac{A_{21}}{A_{21}+A_{23}}\frac{c^2}{8\pi h\nu_0^3}\frac{1}{\Delta\nu_\mathrm{L}}. \tag{6}$$

The laser intensity corresponding to $S=1$ is the saturation intensity defined by

$$I_\mathrm{sat} = \frac{A_{21}+A_{23}}{A_{21}}\frac{8\pi h\nu_0^3}{c^2}\Delta\nu_\mathrm{L}. \tag{7}$$

If $S \gg 1 (I \gg I_\mathrm{sat})$, then

$$n_2(t) \approx n_1(0)\frac{g_2}{g_1+g_2}. \tag{8}$$

By broadband operation of the laser in the saturated regime, the maximum LIF signal is achieved and the optimal signal-to-noise ratio is obtained since the excited population is maximized. In addition, the LIF signal is insensitive to fluctuations in the laser intensity. But, if the laser pulse is too long compared to the lifetime of the excited state, a significant population will be lost to state 3, and $n_2$ will decay away. Despite LIF operation at saturation, a LIF scheme that uses excitation of a metastable state, which is popular in many other experiments, is inadequate for use on PTSX because the density of the metastable state is much smaller. Hence, in PTSX, the LIF schemes that excite the ground state are proposed.

Because of the shiny gold-plated electrodes in PTSX, the detection limit for this scheme will be mainly determined by stray light. A viewing dump can be used to prevent reflected light from entering into the collection optics, and careful designs of the laser dump, windows, filters and baffles are required. In this scheme, $I_\mathrm{LIF}$ can be expressed as

$$I_\mathrm{LIF} \propto \frac{\Omega}{4\pi}An_2V \tag{9}$$

where $\Omega$ is the solid angle of the collection optics, $A$ is the transition rate for the fluorescence line, and the detection volume $V$ is defined as the volume of the laser beam intersected by the collection optics. The intent is to have the detection volume be a cube on the order of with 1 mm side dimensions [13]. In the central section of the trap, the gap between the electrodes is locally enlarged to allow enough field of view for collection optics. For measurement of the ion density at different radial positions, the injection optics and the collection optics will have the capability of translation and tilting. If a CCD camera system is used instead of a Photomultiplier Tube (PMT) or Avalanche Photo Diode (APD), simultaneous measurement along the chord of the laser beam through the plasma can be made.

The 1-D velocity distribution function parallel to the direction of laser propagation ($k\hat{z}$) is defined by

$$f(\mathbf{r}, v_z, t) = \int\int f(\mathbf{r}, v_x, v_y, v_z, t)\mathrm{d}v_x\mathrm{d}v_y. \tag{10}$$

The LIF signal intensity when the laser frequency is tuned to $\omega$ can be expressed as

$$I_\mathrm{LIF}(\omega) \propto f\left(\mathbf{r}, v_z = \frac{\omega-\omega_0}{k}, t\right). \tag{11}$$

This is possible because the laser light seen by an ion moving with velocity $v_z$ is Doppler-shifted according to

$$\omega - kv_z = \omega_0. \tag{12}$$

Hence, by sweeping the laser frequency ($\omega$) across the resonance transition ($\omega_0$), the 1-D velocity distribution function can be measured. To fluoresce a specific ion speed, the spectral width of the laser ($\Delta\nu_\mathrm{L}$) needs to be narrow compared to the Doppler spread of the ions ($\Delta\nu_D$). The Doppler width, $\Delta\nu_D = \frac{\omega_0}{2\pi}\sqrt{8k_\mathrm{B}T\ln 2/mc^2}$, varies from 1.27 to 4 GHz for 493.41 nm transition as the ion temperature in PTSX varies from 0.1 to 1 eV. If the laser intensity is high enough to saturate the transition as in the density measurement, the natural linewidth of the transition ($\delta\nu_n$) will be

Table 1
Proposed LIF schemes for the PTSX

| Initial state | Excited state | Final state | Wavelength (nm) | Transition rate ($A$, $10^6\,s^{-1}$) |
|---|---|---|---|---|
| $6\,^2S_{1/2}$ | $6\,^2P_{1/2}$ | $6\,^2S_{1/2}$ | 493.41 | 96 |
| $6\,^2S_{1/2}$ | $6\,^2P_{1/2}$ | $5\,^2D_{3/2}$ | 649.69 | 33 |

further broadened [11]. Therefore, to measure the Doppler broadening accurately, the laser must be operated in the linear regime, where $S \ll 1$. In the rate equation for $n_2$, if $S \ll 1 (I \ll I_{sat})$, then

$$n_2(t) \approx S \frac{g_2}{g_1} n_1(0). \tag{13}$$

In addition to single-mode operation requirements, the laser should have tuning capability to scan Doppler widths to cover the whole of velocity space. Since, the LIF signal is relatively weak for single-mode linear regime operation, the measurement of the velocity distribution function in PTSX will be very challenging (Table 1).

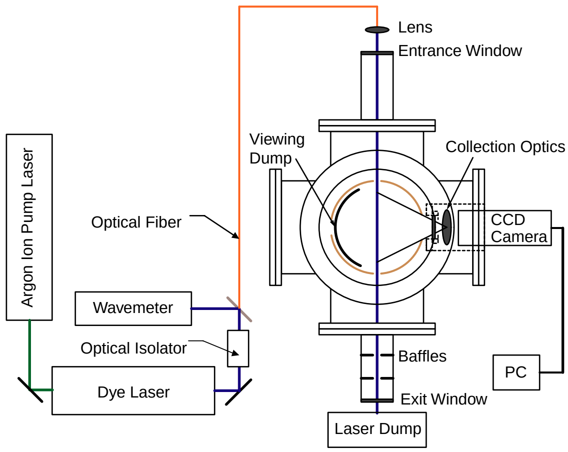


Fig. 2. Schematic diagram of experimental setup.

## 5. Laser system

The laser used in this work is a Coherent 899-21 ring dye laser optically pumped by an argon ion laser, which has been employed for the development of the motional Stark effect with laser-induced fluorescence diagnostic [14]. Coumarian 102 dye is used to excite the 493.41 nm transition. A Burleigh wavemeter is used to measure the output wavelength, and the spectral characteristics are monitored with a Fabry–Perot cavity. A Conoptics optical isolator is inserted in the beam path before coupling to an optical fiber which carries the beam to the experimental apparatus. A Pulnix CCD camera captures the fluorescence image digitally, and the radial density profile can be determined by the intensity of the saved image, with suitable calibration (Fig. 2).

The three-plate birefringent filter allows broadband operation over approximately 2 GHz, which is nearly matched to the Doppler width. For broadband operation with a laser linewidth of 2 GHz, the saturation intensity $I_{sat}$ is about $111.7\,mW/mm^2$ for the 493.41 nm transition. If the laser beam is focused to a cross-section of $1\,mm^2$, a laser power of 111.7 mW is sufficient for saturation. For single-mode operation, the linewidth can be narrowed to 500 kHz with active frequency control. In this case, $\Delta\nu_L \ll \delta\nu_n (= 20.5\,MHz)$ and $I_{sat}$ is about $1.16\,mW/mm^2$ for the 493.41 nm transition. By continuously varying the cavity length with the rotating galvanometer-driven Brewster plate, a single-mode tuning capability up to 30 GHz is also possible, which can cover many Doppler widths and is adequate for the ion velocity distribution function measurement. The laser output power is high enough for both broadband operation and single-mode operation.

## 6. Summary and future plan

In summary, a laser-induced fluorescence diagnostic system is under development for the nondestructive measurements of the ion density profile and the ion velocity distribution function in the PTSX device. In PTSX, by spoiling the waveform of the bias potential, the effects of beam mismatch on emittance growth and halo particle production can be investigated. The density profile measurement with sufficiently long integration times will allow for the detection of the halo particles, and the velocity–space measurements will provide information on beam emittance. Because the ion density of the PTSX is very low ($\sim 10^5$ particles/cm$^3$), technical issues such as suppressing stray and reflected light must be resolved in order to obtain meaningful data.

## Acknowledgements

This research was supported by the U.S. Department of Energy. The authors would like to thank Mr. A. Carpe for his excellent technical support, and Ms. E.L. Foley for useful discussions and help in the development of the laser system.

## References

[1] R.C. Davidson, H. Qin, Physics of Intense Charged Particle Beams in High Intensity Accelerators, World Scientific, Singapore, 2001.
[2] H. Okamoto, H. Tanaka, Nucl. Instr. and Meth. A 437 (1999) 178.
[3] R.C. Davidson, H. Qin, G. Shvets, Phys. Plasmas 7 (2000) 1020.
[4] E.P. Gilson, R.C. Davidson, P.C. Efthimion, R. Majeski, Phys. Rev. Lett. 92 (2004) 155002.
[5] T.W. Koerber, M.H. Schacht, K.R.G. Hendrikson, W. Nagourney, E.N. Fortson, Phys. Rev. Lett. 88 (2002) 143002.
[6] E.P. Gilson, R.C. Davidson, P.C. Efthimion, R. Majeski, E.A. Startsev, American Institute of Physics Conference Proceedings 692 (2003) 211.
[7] R. Schrittwieser, R. Koslover, R. Karim, N. Rynn, J. Appl. Phys. 58 (1985) 598.
[8] I. Katsumata, M. Yamasaki, K. Murakami, M. Fujimoto, H. Tsukahara, Y. Nanjo, H. Yoshimura, Rev. Sci. Instrum. 65 (1994) 1392.
[9] K. Muraoka, M. Maeda, Laser-aided Diagnostics of Plasmas and Gases, Institute of Physics Publishing, Bristol, 1999.
[10] D.J. Wineland, Science 226 (1984) 395.
[11] W. Demtroder, Laser Spectroscopy, Springer, Berlin, 2002.
[12] C.D. Zuiker, Laser-induced fluorescence measurements in an electron-cyclotron resonance plasma etch reactor, Ph.D. Dissertation, Princeton University, 1993.
[13] R.C. Davidson, P.C. Efthimion, R. Majeski, H. Qin, G. Shvets, Nucl. Instr. and Meth. A 437 (2001) 502.
[14] E.L. Foley, F.M. Levinton, Proceedings of the 15th Topical Conference on High-Temperature Plasma Diagnostic, 2004, in press.